Low-Rank Sum-of-Products Finite-Basis-Representation (SOP-FBR) of Potential Energy Surfaces

Ramón L. Panadés-Barrueta[1] and Daniel Peláez[2,*]

[1]*Laboratoire de Physique des Lasers, Atomes et Molécules (PhLAM), Université Lille 1, Villeneuve d'Ascq cedex, France.*

[2]*Institut des Sciences Moléculaires d'Orsay (ISMO) - UMR 8214. Bât. 520, Université Paris-Saclay, 91405 Orsay Cedex*

(Dated: November 27, 2020)

Abstract

The SOP-FBR approach for the automated multidimensional fit of potential energy surfaces (PES) is presented. In its current implementation the method yields a PES in the so-called Tucker sum-of-products form but it is not restricted to this specific *ansatz*. The novelty of our algorithm lies in the fact that the fit is performed in terms of a direct product of *Schmidt* basis, also known as *natural potentials*. These encode in a non-trivial way all the physics of the problem and, hence, circumvent the usual extra *ad hoc* and *a posteriori* adjustments (*e.g.* damping functions) of the fitted PES. Moreover, we avoid the intermediate *refitting* stage common to other tensor-decomposition methods typically used in the context of nuclear quantum dynamics. The resulting SOP-FBR PES is analytical and differentiable *ad inifinitum*. Our *ansatz* is fully general and can be used in combination with most (molecular) dynamics codes. In particular, it has been interfaced and extensively tested with the Heidelberg implementation of the Multiconfiguration Time-Dependent Hartree (MCTDH) quantum dynamical software package.

*Electronic address: Daniel.Pelaez-Ruiz@universite-paris-saclay.fr

I. INTRODUCTION

Major advances in the field of quantum dynamics have been connected to the introduction of novel *ansätze* for the efficient representation of multidimensional objects, the wavefunction (WF) being the most distinguished member of this category. Indeed, a major breakthrough took place with the introduction of the Multiconfiguration Time-Dependent Hartree (MCTDH) method[1]. In MCTDH the WF is represented by an efficient two-layer adaptive scheme consisting on a time-dependent nuclear basis set expressed in terms of a time-independent one. This allowed, for the first time, to overcome the traditional *4-atom limit* of the so-called *standard* method when considering quantum dynamical problems using non-analytical potentials. Perhaps, the most relevant change of paradigm arrived with the adoption of a multilayer (tree) formalism epitomized by the Multilayer MCTDH (ML-MCTDH)[2–4] which was subsequently adopted by related methods such as the Gaussian variants of MCTDH.[5,6] These compact and highly flexible multilayer-tree structures have allowed the implementation of very efficient iterative[7] and recursive algorithms.[4,8] More recently, a new generation of promising methods in which the object structures belong to the Tensor-Train family have appeared.[9–12]

A common feature to all these methods is that they are particularly suited or rely exclusively on Hamiltonian operators expressed in a separable form, the so-called sum-of-products (SOP) form, such as the Vibronic Coupling model Hamiltonian. Considering the Kinetic Energy Operator, either it is already in this form or it can be expressed either analytically[13] or numerically[14] in SOP form in a *quasi* automated fashion. On the other hand, the computation of potential energy surfaces (PESs) still poses major challenges. For decades now, major efforts have been devoted to the development of efficient tensor decomposition algorithms to turn these *a priori* unstructured objects (multidimensional PES) into separable form.[15–20] A common feature to all these methods is that they rely on a two-step *decoupled* scheme. After the multidimensional fit of a set of *ab initio* energies, the resulting PES is tensor decomposed to achieve the sought separable form. An exception to this can, in a certain sense, be found in the so-called *on-the-fly* methods in which a more or less local (in configuration space) PES is obtained directly from electronic structure calculations.[21]

In this work, we shall introduce a scheme for the computation of a *global* PESs directly

from electronic structure calculations in separable form, more specifically, but by no means restricted to, the Tucker SOP form. The computation of a more or less *global* high-dimensional PESs is a laborious task involving the calculation of energies and possibly properties in a large set of reference configurations, followed by the fit into an analytic expression. The latter will be turned into a *hopefully* efficient code which will be interfaced with or directly implemented in a dynamics software package. Assuming the possibility of numerically converged dynamical calculations, one can conclude that two major factors will contribute to the quality of a simulation: (i) the accuracy and adequacy of the underlying electronic structure calculations (*i.e.* combination of level of theory and electronic basis set); (ii) the errors associated to the fitting procedure which, in turn, depend on the adequacy of the distribution of the reference geometries. In addition to this, as already mentioned above, the use of PES in combination with grid-based quantum dynamical methods, like MCTDH,[1] does greatly benefit from PESs expressed in SOP form. Consequently, an extra tensor decomposition stage with its intrinsic error (see for instance Ref.[16]) should be added to this workflow.

There is a plethora of fitting procedures for PESs available, so we refer the reader to (part of) the original and extensive literature.[22–27] We will, however, turn our attention into methods which, by *ansatz*, directly provide a SOP form (Eq.1). In this category, we can distinguish three types of methods: (i) those providing a local (Taylor) expansion, typically Quartic Force Fields;[28–30] (ii) those using an appropriate Neural Network (NN) approach (epitomized by the seminal work of Manzhos and Carrington[31] and recent applications thereof)[32,33]; and (iii) those directly fitting into a separable form (see for instance,[9,20,34–38]) including specific NN *ansätze* which have been shown to be directly expressible in separable form.[31,32] It is worth highlighting the efficient combination of a Smolyak quadrature with non-direct product basis achieved by Ávila and Carrington.[37] Perhaps, a more particular case of this last category is given by our recent method for global multidimensional fit of PES[20] in which an intermediate and inexpensive (yet chemically accurate) representation of the electronic Hamiltonian (a reparametrised semiempirical Hamiltonian) can be directly interfaced to a tensor decomposition method such as the Multigrid POTFIT algorithm,[16] hence the name of the method Specific Reaction Parameter Multigrid POTFIT (SRP-MGPF).[20] In this regard, the physically meaningful representation of the SRP Hamiltonian

allows for the use a fairly small amount of reference points while, at the same time, it provides a physically correct PES.[20] The quality of this SRP PES has been assessed through the determination of accurate vibrational eigenstate and the propagation of a wavepacket using the MCTDH software.

As briefly sketched above, in (molecular) quantum dynamics (*aka* multidimensional wavepacket propagations) arguably the main bottleneck is the computation and representation the potential energy surface (PES) in a suitable form.[16,20] Turning our attention to MCTDH, a potentially numerically exact method, an already existing PES (in the form of a subroutine or an appropriate analytical function) has to be preprocessed (tensor decomposed) in order to achieve the so-called sum-of-products (SOP) form representation:

$$V = \sum_r c_r \prod_\kappa v_r^{(\kappa)} \tag{1}$$

where the $v^{(\kappa)}$ are mono- (or low-dimensional) basis functions expressed on a grid (see Eq.3). There are plenty different types of SOP forms (Tucker form, CP format, Tensor-Train decomposition or even the conceptually simple Taylor expansion, among others). In this work, we shall focus on the so-called Tucker form (Eq.3) which is the most commonly used in MCTDH. The reader is referred to the abundant literature concerning the advantages of using SOP in general (curse of dimensionality, quadrature) and in MCTDH in particular (see for instance the *classical* MCTDH Review).[1] It should be stressed that the subsequent discussion is fully general and thus applicable to any type of multidimensional functions. However, without any loss of generality, we shall make reference to aspects related to MCTDH quantum dynamics.

The different *variational* Tucker decomposition schemes proposed over the years[15–17] have been shown to be efficient, accurate, and, most relevantly, they have been shown to allow a systematic control of the error owing to their variational character. In all of these methods, the main goal is to compute an accurate representation of (or an approximation to) potential density matrices from which grid-based *Schmidt* basis functions (*aka* single-particle potentials, natural potentials) can be extracted as eigenvectors. The main difference in these methods is simply how they arrive to these density matrices. For instance, in the pioneering POTFIT algorithm,[15] this was achieved by computing the

potential on the whole grid (thence its power but limited applicability). On the other hand, in Multigrid POTFIT,[16] this was achieved using a series of nested grids, whereas in the equivalent Monte-Carlo POTFIT,[17] the potential density matrices were stochastically approximated. For the sake of completeness, we should at this point mention the powerful strategies proposed by Otto[18,19] and Schröder[39] in which the sought separable form is obtained through a series of (recursive) High-Order Singular Value Decompositions[40] and a CANDECOMP[41,42] formalism, respectively. In any case, the common requirement of all these approaches is the *preexistence* of a PES in analytical form. Consequently, they can be seen as *refitting* methods.

In this work, we tackle this very problem under the assumption that it is possible to achieve a SOP form directly from high-level electronic structure calculations. As it will be shown, this makes the computation of a global PES more efficient and, what is more relevant, less prone to errors since this scheme reduces the necessary number of stages to this end. As such, our sum-of-products Finite-Basis-Representation (SOP-FBR) approach, constitutes an alternative to some NN-based methods.[31,32] The idea behind SOP-FBR is simple. Given a low-rank Tucker expansion on the grid, we replace the grid-based basis functions (*i.e.* natural potentials) by an expansion in terms a set of functions. As a result, a global SOP-FBR PES is simply an analytical expression in Tucker form (but not restricted to this specific form). The SOP-FBR parameters are obtained by optimisation using an appropriate number of reference *ab initio* energies. A subtle difference between SOP-FBR and any traditional multivariate regression method is the fact that we do not directly fit our PES to, say, a set of physically-oriented polynomials (*one-layer*). In SOP-FBR, we optimize a certain number of configuration interaction coefficients together with the expansion coefficients necessary to expand optimal *Schmidt* basis (*i.e.* natural potentials) in terms of a given set of functions (*e.g.* orthonormal polynomials). Consequently, SOP-FBR relies on a *two-layer* scheme, analogous (no time-dependence though) to the MCTDH one in which the WF is represented by a time-dependent basis (upper layer) and an underlying time-independent one (lower layer). This scheme provides us with a highly flexible model relying on the *optimal* properties of a multidimensional Schmidt decomposition (see Appendix D in[1] and Appendix B in[16]).

II. THEORY

The *traditional recipe* for the preparation of a PES suited for quantum dynamical calculations typically implies three/four steps:

1.- the judicious choice of reference geometries;

2.- the computation of accurate reference energies;

3.- an analytical fit; and

4.- (in certain cases) a tensor decomposition.

With respect to step 1, we have recently shown that it is possible to automatically obtain an *optimal* set of pivotal structures (based on the stationary points) from which systematically generate a set of reference geometries.[20] On the other hand, from step 2, all stages imply a direct loss of quality in the resulting PES owing to: (i) the intrinsic accuracy of the selected level of theory; (ii) the accuracy of the fit (dramatically dependent on the dimension of the system); and (iii) the quality of the decomposition, which is directly related to the size of the resulting expansion and the quality of the basis functions. To understand the last point, one should simply consider the vast configuration space associated to the parametrical representation of the chosen tensor structure. In this respect, multiple minima are to be expected owing to the usual non-unique character of a, for instance, Tucker decomposition.[43] Since our approach involves (but it is by no means limited to) Tucker expansions, in the following we shall use the terms SOP and Tucker exchangeably.

We propose to combine stages 3 and 4 in a single step thus, potentially (and effectively) reducing the number of steps involved in a PES fit together with the concomitant errors. Obviously, electronic structure calculations are unavoidable, so far, but owing to the computer power available (*e.g.* supercomputer centers), this is not anymore a *bottleneck*. The basic idea is that it is possible to arrive to an *optimal* SOP (Tucker) expression (*i.e.* to the optimal parameters defining it) either stochastically or by using some kind of, possibly global, optimization algorithm. In other words, a guess of initial SOP parameters will be optimised according to a suitably defined target function. In our case, this will be the root-mean square error (RMSE, $\chi(\mathbf{Q})$) between the reference function (*exact*) and our current

approximation to it (*app*):

$$\chi(\mathbf{Q}) = \sqrt{\frac{\sum_i^N \Delta V_i^2(Q_i)}{N}} \tag{2}$$

where $\Delta V_i = V^{exact}(Q_i) - V^{app}(Q_i)$ is the difference between the exact potential and the approximated one at the i-th reference geometry. Ideally, the approximation should be such that when computing the RMSE using another (possibly denser) set of geometries ($\{\mathbf{Q}'\}$, validation set) different from the reference one, the RMSE remains reasonably close to the reference one: $|\chi(\mathbf{Q}) - \chi(\mathbf{Q}')| < \epsilon$ with ϵ small.

At this point, it should be emphasised that in contrast to grid-based tensor decomposition methods, in SOP-FBR we do not necessarily rely on a grid. The so-called single-particle (or natural) potentials of POTFIT (or related methods) are replaced by analytical functions which we refer to as *Schmidt* functions. The latter are expanded in a given polynomial series (Chebyshev in our case). This results in a set of parameters (*core* tensor and expansion coefficients) which are optimised in order to reproduce a given level of theory. To obtain a suitable guess for the optimisation process, we employ an initial (grid-based) Tucker decomposition using, for instance, the Higher Order Orthogonal Iteration (HOOI) algorithm as implemented in the `TensorLy` library. It should be stressed that this initial decomposition cannot be directly performed on the high-level PES (e.g. high-level ab initio) owing to the huge number of grid points needed and the necessary CPU time for this. This has been extensively discussed in our previous work on SRP-MGPF.[20]

A low-rank f-dimensional grid-based expansion of the PES in Tucker form reads:

$$V^{app}_{i_1,i_2,\ldots,i_f} = \sum_{j_1}^{m_1} \cdots \sum_{j_f}^{m_f} C_{j_1,\ldots,j_f} \prod_{\kappa}^{f} v^{(\kappa)}_{i_\kappa j_\kappa} \tag{3}$$

where $C_{j_1,\ldots,j_f}$ is a coefficient belonging to the so-called *core* tensor and $v^{(\kappa)}$ are the *Schmidt* basis functions (factor matrices in the tensor community[44]) expressed on a grid (note the two indices).[15] The latter are referred to as single-particle potentials (SPPs) in the MCTDH literature. This is the *ansatz* commonly used in POTFIT, MGPF or MCPF to represent the PES in SOP form. In this expression, the PES value at a given geometry (V($\mathbf{Q}$), with $\mathbf{Q} \equiv \left(q_{i_1}, \ldots, q_{i_f}\right)$) specified by its grid indices $((i_1, i_2, \ldots, i_f) \leftrightarrow \left(q_{i_1}, \ldots, q_{i_f}\right)$) is expressed as a sum of products of weighing coefficients ($C_{j_1,\ldots,j_f}$) times a (Hartree) product of one- (or

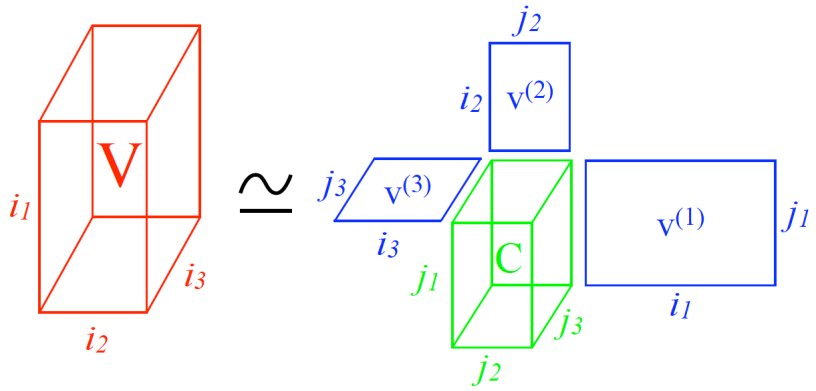

FIG. 1: Graphical representation of a 3D Tucker expansion. See main text for explanation.

low-) dimensional functions on a grid ($v^{(\kappa)}_{i_\kappa j_\kappa}$). Note that by κ we refer to a given degree of freedom (DOF). In Figure 1, we display the graphical representation of a 3-dimensional (3D) Tucker expansion. Note that the *core*-tensor has the same dimensionality than the initial reference tensor of PES on the grid and thus it is affected by the curse of dimensionality at the same rate. With respect to notation, the above Tucker expression can be more compactly written as (see Kolda and Bader's comprehensive review)[43]:

$$V^{app} = [\![\mathcal{C}, \mathbf{v}]\!] \tag{4}$$

To motivate our discussion, we should recall that in the original POTFIT (and related methods), the SPPs are grid-based basis functions adopting the form of matrices. Hence the SPPs merely contain the collection of SPP values at the grid points. Consequently, the existence of implicit *underlying SPP/Schmidt functions* can be exploited in order to increase the density of the grid representation of PES. In MCTDH, this is the so-called `chnpot` procedure in which some kind of interpolating procedure (*e.g.* cubic splines) is used to approximate SPPs values in the regions in between the original grid points.[15] The SPPs or Schmidt functions are smooth except perhaps for the large j ones. To illustrate this, we present in Figure 2 the first 10 SPPs of the water molecule (see details of the PES later in text) on a grid (dots) together with interpolating functions (lines). The SPPs have been obtained through the Higher Order Orthogonal Iteration (HOOI) method as implemented in the `TensorLy` Python library.[45]

As it can be observed, there is a remarkable smoothness in the lower-j basis functions whereas the higher-j SPPs exhibit a highly oscillating (somewhat noisy) and, hence, unde-

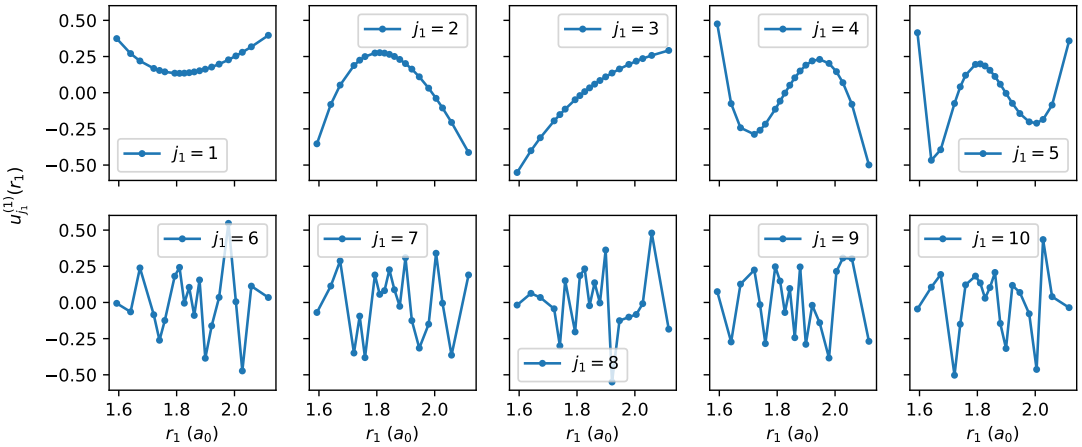

FIG. 2: Representation of the first 10 natural potentials of the PJT2-PES of the H_2O molecule. The dots represent the values of the natural potentials at the DVR grid points.

sirable trend for fitting. At this point, it should be further emphasised that these lower-j Schmidt basis carry the most relevant information of the PES as proven by the fact that grid-based methods such as MGPF or MCPF only require such a small amount of SPPs. The behaviour of the SPPs was already discussed in the seminal POTFIT paper by Jäckle and Meyer[15] as well as by Manzhos and Carrington.[46] Interestingly, this important property has not been fully exploited and lies at the core of our approach. Based on this simple observation, we propose a new low-rank *ansatz* in which we substitute the SOP grid-based expression (Eq.3) by a SOP Finite Basis Representation (SOP-FBR) in terms of some basis functions ($T(q)$):

$$V(q_1, \ldots, q_f) = \sum_{j_1}^{m_1} \cdots \sum_{j_f}^{m_f} C_{j_1,\ldots,j_f} \prod_{\kappa}^{f} (\sum_{\mu}^{t_\kappa} c_{\mu,j_\kappa}^{(\kappa)} T_\mu(q_\kappa)) \tag{5}$$

where the the grid indices (i_κ) in Eq.3 have been replaced by the value of the actual coordinate (q_κ). This expression can be used in any grid since the grid-based SPPs ($v^{(\kappa)}$) are now interpolated through the use of a weighted sum of t_κ T-basis functions:

$$v_j^{(\kappa)}(q_\kappa) = \sum_{\mu}^{t_\kappa} c_{\mu,j_\kappa}^{(\kappa)} T_\mu(q_\kappa) \tag{6}$$

with T assumed to be appropriated for the specific problem. The case we discuss is that of a general molecular PES (multiwell bound region) for which the typical behaviour is that of

the SPPs in Figure 2. However, we have observed that the higher-j SPPs for the Coulomb potential present a convoluted sinus type behaviour (work in progress). Throughout this work we have expressed T with Chebyshev polynomials but any other functions are also possible. Consequently, this change in the representation, from grid to FBR, leads to a full analytical global PES, grid-independent and differentiable *ad infinitum*. Indeed, one can immediately realise that n-th order derivatives can be obtained in a straightforward manner. By direct differentiation, one obtains:

$$\frac{\partial^n V(q_1, q_2, \ldots, q_f)}{\partial q_\kappa^n} = \sum_{j_1}^{m_1} \cdots \sum_{j_f}^{m_f} C_{j_1,\ldots,j_f} \left(\sum_{\mu}^{t_\kappa} c_{\mu,j_\kappa}^{(\kappa)} \frac{\partial^n T_\mu(q_\kappa)}{\partial q_\kappa^n} \right) \prod_{\nu \neq \kappa}^{f} \left(\sum_{\mu}^{t_\nu} c_{\mu,j_\nu}^{(\nu)} T_\mu(q_\nu) \right) \quad (7)$$

At this point it is convenient to highlight some analogies between low-rank grid based methods, such as grid-based MGPF and grid-free SOP-FBR. In the original publication[16] and subsequent applications,[47–49] it could be observed that MGPF is able to extract a very compact representation of the PES following a given prescription in the choice of the reference points (see discussion on the sparsity of the *core* tensor in Section III B). For instance, in Ref.[48], the infrared spectrum of $H_3O_2^-$ (9D) was computed. The MGPF PES required 1.7 MB of storage. In contrast, the original PES which would have required 10^5 MB. The resulting MGPF PES based spectrum was in good agreement with the reference experimental Ar-vibrational predissociation one. In view of the nice agreement, discrepancies between both spectra could be attributed to the effect of the Ar atom in the vibrational structure of the $H_3O_2^-$ complex. In other words, considering the PES as a multidimensional image, it is possible to compress it using just a few basis functions. The difference in SOP-FBR is only that we achieve the same expansion through an extra parametrization of the SPP (Schmidt functions) and an optimisation. In summary, it is possible to obtain such an $\mathcal{L}^2$-optimal Tucker expansion using numerical methods such as stochastic, global, local search algorithms or a suitable combination thereof.

To finalize this Section, for the MCTDH oriented reader, we would like to point out that the *contracted* mode (ν):[15]

$$D^{(\nu)}_{j_1\ldots i_\nu \ldots j_f} = \sum_{j_\nu} C_{j_1\ldots j_\nu \ldots j_f} v^{(\nu)}_{i_\nu j_\nu} \quad (8)$$

can be readily obtained from a SOP-FBR expression through:

$$D^{(\nu)}_{j_1\ldots i_\nu \ldots j_f} = \sum_{j_\nu} C_{j_1\ldots j_\nu \ldots j_f} v^{(\nu)}_{j_\nu}(q^{(\nu)}_{i_\nu}) \quad (9)$$

provided that a large enough sampling has been considered for the contracted mode (*cf.* torsion mode in HONO in Section III B).

III. RESULTS AND DISCUSSION

In this Section, we shall introduce and discuss the actual implementation of the method as well as the computational and numerical properties of the SOP-FBR PES. Hereafter, the following notation for our SOP-FBR expansions will be used: $[(m_1, t_1), (m_2, t_2), (m_3, t_3), ...]$ representing an f-dimensional *core* tensor possessing $\prod_{\kappa}^{f} m_\kappa$ elements. This also indicates that each κ DOF is given by a set of m_κ basis functions which, in turn, are expressed in terms of t_κ underlying basis, in the present case, Chebyshev polynomials. It should be further emphasized that there is no restriction in the type of basis sets employed, except that it should be adapted to the target potential. The total number of parameters will formally then be: $\prod_{\kappa}^{f} m_\kappa + \sum_{\kappa}^{f} m_\kappa \cdot t_\kappa$. As it will be discussed, we will profit from the huge range of values (over 12 orders of magnitude) among the *core* tensor elements to greatly reduce the number $\prod_{\kappa}^{f} m_\kappa$ terms.
Finally, in those cases where d DOF are represented by the same amount of basis functions, we shall simply write $[d \times (m, t)]$. Note that the Chebyshev polynomials start at order 0, hence (m, t) implies the use of a Chebyshev polynomial of maximum order $(t - 1)$.
It should be stressed that all reference data (particularly, vibrational eigenenergies) to which we compare our SOP-FBR results, have been computed by ourselves with MCTDH using the corresponding PES routine.

A. SOP-FBR of a low-dimensionality PES: H_2O (3D)

In the following section, we shall tackle a *realistic* 3D problem, the water (H_2O) molecule. We have used the Polyanski-Jensen-Tennyson $H_2^{16}O$ spectroscopically refined PES known as PJT2.[54]

1. Generation of the guess parameters

In order to start our calculation with a physically oriented guess, we have used an inexpensive SRP PES computed *a priori* following our recent method[20] using our own software (SRPTucker[55]) which is interfaced with the MOPAC semiempirical software.[56] This SRP PES can be readily decomposed on a grid using the High Order Orthogonal Iteration (HOOI) algorithm[43] thus obtaining an initial *core* tensor and its associated Schmidt basis functions (SPPs). In this particular SRP PES, we utilised a grid of 5^3 reference geometries (a subset of the one that we use for the SOP-FBR optimisation) and made use of the Parametric Model 3 (PM3) Hamiltonian.[57]

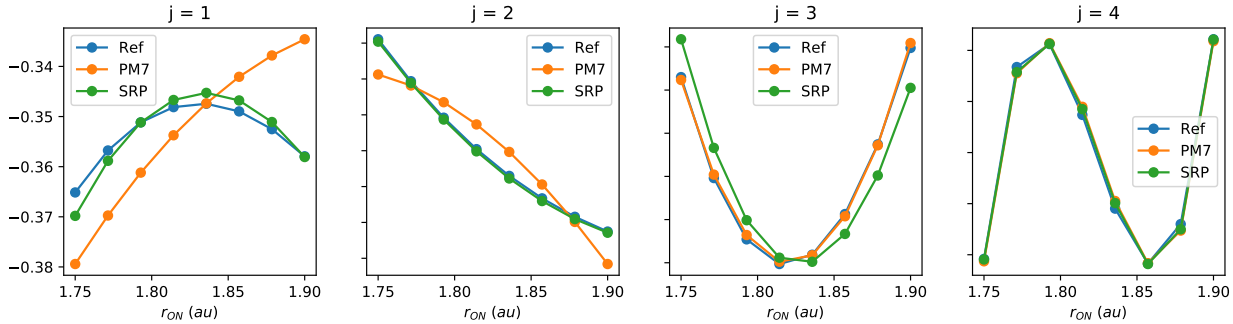

FIG. 3: First five SPPs of the angular DOF (θ_{HOH}) for the H_2O molecule obtained by HOOI Tucker decomposition using (i) the reference potential PJT2[54] (blue) (ii) the PM3 Hamiltonian (orange); and (iii) the resulting SRP (green).

Figure 3 displays a comparison of the first five SRP SPPs for the *ab initio* reference surface, the PM3 surface, and the resulting SRP. As it can be observed, the guess SRP SPPs are in much better agreement with the *exact* ones than the original PM3. From these plots, we notice that the SRP constitutes a better source of guess parameters than the PM3 method. Despite the fact that we are dealing with guess (initial) Schmidt functions (SPPs), any improvement in the shape of the semiempirical SPPs will be turned into a saving in computational effort when searching for the optimal SOP-FBR solution. On the other hand, the most relevant elements of the *core* tensor are very similar for the three methods (see Figure 4).

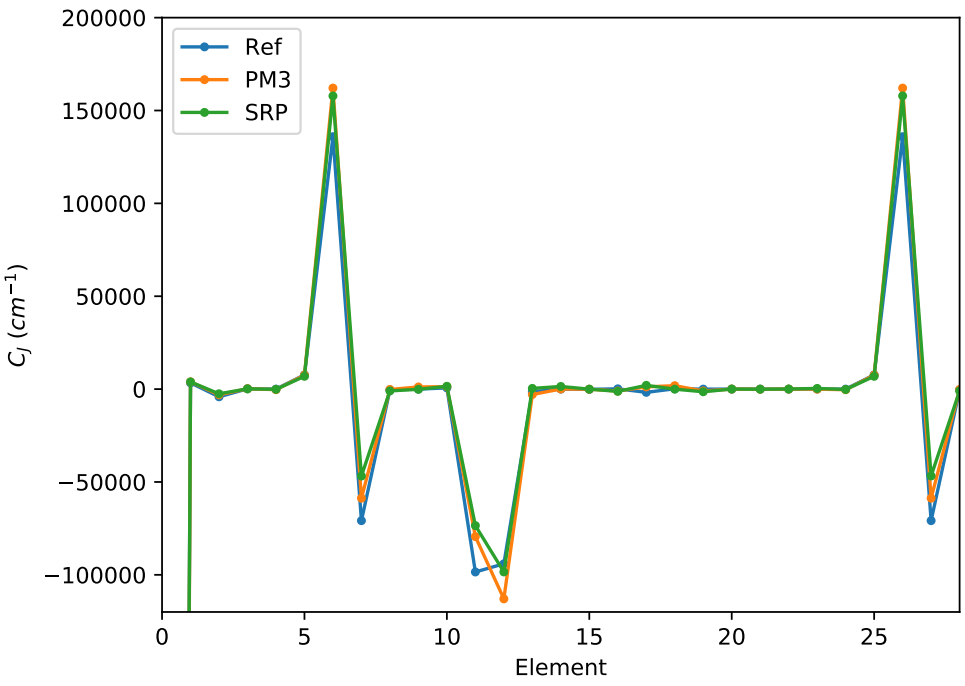

FIG. 4: Comparison of the first elements of the *core* tensor of the H_2O molecule obtained by HOOI Tucker decomposition of (i) the reference potential[54] (ii) the PM3 hamiltonian and (iii) the corresponding SRP. Since the *core* tensor happens to be very sparse, for higher index values the differences are even less appreciable.

For the sake of efficiency, prior to any optimisation, we have imposed a symmetrization by *ansatz* to the SOP-FBR expression: (i) the SPPs for both OH stretching modes have been forced to be equal, and (ii) the *core* tensor elements satisfy the $C_{ijk} = C_{jik}$ condition, where ijk are indices referring to Schmidt basis functions (SPPs) and we have implicitly assumed the $[r_1 \equiv \nu_{OH1}, r_2 \equiv \nu_{OH2}, \theta_{HOH}]$ mode ordering. It should be noticed that if no such restriction is imposed, the obtained SPPs are nevertheless reasonably close to the symmetrized ones.

The SOP-FBR optimisation has been performed in a *decoupled* manner using a combination of global and local algorithms, namely Multi-Level Single-Linkage (MLSL)[58] for the former and Bound Optimization BY Quadratic Approximation (BOBYQA) for the latter.[59] This type of approaches have been shown to be very well adapted to the reparametrisation of semiempirical Hamitonians.[20] For this optimisation, we used a set

(grid) of [15, 15, 15] structures (mode ordering as above) and the SOP-FBR structure was $[3 \times (5, 11)]$ thus generating a parameter space of size $5^3 + 3 \cdot 5 \cdot 11 = 290$. The reference points were generated through homogeneous sampling of normal distributions centred at the water molecule equilibrium parameters. We used for this the `truncnorm` method of SciPy.[52] The standard deviation was set up in order to cover the 1D intervals taken from the MCTDH model inputs, which are available in the Heidelberg MCTDH software package (see Table II). It should be stressed that equilibrium geometrical parameters can be computed through the use of automated methods (see for instance Ref.[60] and references therein).

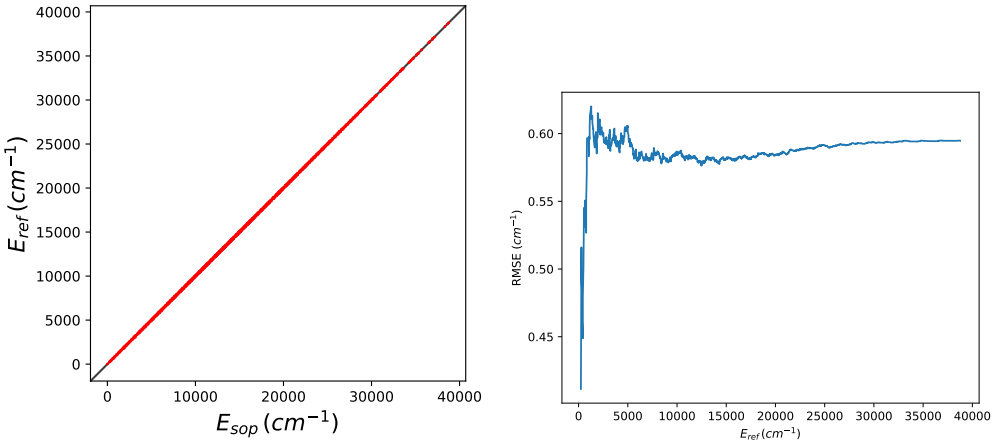

FIG. 5: Correlation plot between the reference *ab initio* energies and corresponding SOP-FBR energies, and cumulative RMSE values obtained with a reference tensor of $15 \times 15 \times 15$ points.

The resulting SOP-FBR RMSE was of 0.686 cm^{-1}, a value which was nicely preserved (0.703 cm^{-1}) when considering a validation set of 10^6 points, different from the reference ones. It should be noted that similar errors have been obtained with larger sets, all converging to the reference value (HOOI decomposition) of RMSE = 0.673 cm^{-1}. The quality of the resulting SOP-FBR PES has been assessed in several different ways. In Figure 5, we present a graphical analysis of its quality in the form of a correlation plot between the reference and SOP-FBR energies (left panel) and the cumulative RMSE (right panel). As it can be observed, the error is equally distributed along the whole energy interval [0, 40000] cm^{-1}. Moreover, we have computed the minimum of the PES using the steepest descent method. The SOP-FBR and reference values (see Table I) agree up to the fourth decimal place.

TABLE I: Minimum geometrical parameters for the reference PES and the SOP-FBR PES obtained with the steepest descent algorithm. Distances are in atomic units and angles are in radians.

PES	$\mathbf{r_1}$	$\mathbf{r_2}$	$\boldsymbol{\theta}$
Ref.	1.8102	1.8102	1.8238
SOP-FBR	1.8102	1.8102	1.8240

As final test of the quality of the SOP-FBR PES, we have computed the Zero Point Energy (ZPE) and lowest vibrational eigenvalues with the MCTDH algorithm. For this problem, we have considered the Discrete Variable Representation (DVR) shown in Table II.

TABLE II: Definition of the MCTDH DVR primitive grid for the water molecule. Stretching motions (ν_{OH}) are represented by r_i ($i = 1, 2$) and the HOH bending by θ. The DVR basis functions are sinus (sin) for the former and Legendre (Leg) DVR for the latter. N is the number of primitive (DVR) grid points. The range represents the first and last grid points in atomic units for the distances and in radians for the angle. The contracted mode is the angle.[16]

DOF	**DVR**	**N**	**Range**
r_1	sin	34	[1.4500, 2.4500]
r_2	sin	34	[1.4500, 2.4500]
θ	Leg	50	[1.1400, 3.1416]

Our results are in very nice agreement with the reference PES. Our ZPE is of 4660.225 cm^{-1}, a value which nicely compares to the reference POTFIT value of 4660.124 cm^{-1}. It should be noticed that the grid-size used in both MCTDH calculations (SOP-FBR and POTFIT) is probably not large-enough so that our eigenvalues are not of the highest-quality (out of the scope of this work). Consequently, the reader interested in more precise results should refer to dedicated studies.[54] The remaining vibrational eigenvalues (relative to the ZPE) are presented in Table III. In all cases, the differences between the SOP-FBR and the reference values is below 1 cm^{-1}.

TABLE III: Comparison of the 20 lowest vibrational eigenvalues of H_2O for the original PES and the SOP-FBR one.

State	**Eigenenergies (cm^{-1})**	
	SOP-FBR	**Reference**
0	0.	0.
1	1593.261	1593.624
2	3151.076	3151.074
3	3722.318	3722.315
4	3820.802	3820.786
5	4670.742	4670.669
6	5297.252	5297.631
7	5394.652	5395.063
8	6150.238	6150.351
9	6839.599	6839.602
10	6938.042	6938.046
11	7452.389	7452.381
12	7572.758	7572.731
13	7584.352	7584.555
14	7644.830	7644.798
15	8345.769	8345.688
16	8450.176	8450.059
17	8949.339	8949.394
18	9010.874	9011.259
19	9136.455	9136.860
20	9204.255	9204.683

B. Six dimensional case: HONO isomerization

As final example, we study now the HONO (6D) PES in the *cis-trans* isomerization region which has become a benchmark for these type of methodological studies.[9,20,32] In this

case the reference PES is given by the model CCSD(T)/cc-pVQZ-quality analytical PES of Richter *et al.*[61] The structure of our 6D SOP-FBR PES is given by $[5 \times (5,7),(12,12)]$, that is, 5 Schmidt basis (SPPs) represented by 7 Chebyshev polynomials each, for all DOF except the torsion which necessitates a somewhat larger basis (*i.e.* sampling) of 12 Schmidt basis (SPPs) represented by 12 Chebyshev polynomials each (up to 11th order).

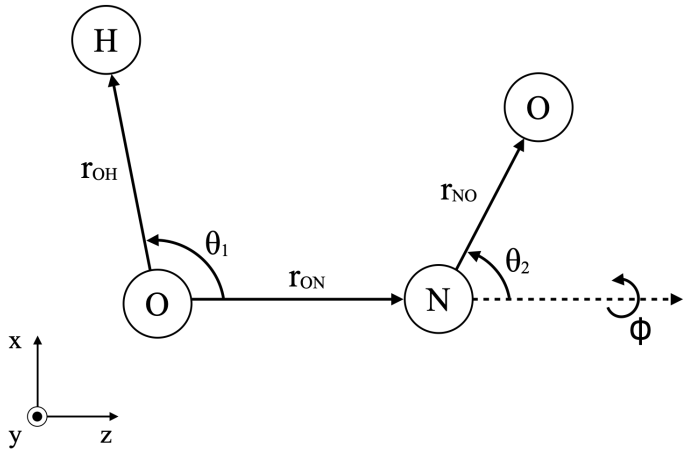

FIG. 6: Definition of the internal coordinates of HONO.

For the SOP-FBR (decoupled) optimisation, we have used the BFGS algorithm in combination with a set of 37500 reference geometries, mapped onto a [5, 5, 5, 5, 5, 12] Cartesian product grid of reference energies. The DOF ordering is $[r_{OH}, r_{NO}, u_2, r_{ON}, u_1, \phi]$ (see Table IV). The intervals of definition of the different DOF can be found in Table IV). For the sake of comparison, we have defined $u_i = \cos\theta_i$ (i=1,2) as in previous studies.[20,61]

Our strategy to initialize our SOP-FBR optimisation has consisted again in generating a guess *core* tensor and the associated set of SPPs using the HOOI decomposition (same structure of our target SOP-FBR) using a SRP PES. For the latter, we have chosen the so-called $\{\zeta_{1084}\}$ set of SRP-parameters which we generated for the title system and which showed an accurate vibrational structure (see Ref.[20] for more details). In Figure 7, we display a comparison of the first four SPPs for selected DOF (a distance, an angle, and the torsion), r_{NO}, u_1 and ϕ, respectively. As in the case of water, the SRP SPPs are closer to the reference ones, in turn, leading to a higher efficiency in the SOP-FBR optimisation.

TABLE IV: Definition of the MCTDH primitive grid for HONO (6D). Discrete Variable Representation (DVR) basis functions are: HO, harmonic oscillator (Hermite) and cos, cosine functions. N is the number of primitive (DVR) grid points. The range in each case is given the first and last grid points in atomic units for the distances and ϕ is the torsion angle in radians. Cosines of the valence angles have been defined: $u_i = \cos\,\theta_i$ (i=1,2). The DOF representation is given in Figure 6. Physical modes have been combined into logical ones as follows: [ϕ], [r_{OH}] [u_2, r_{ON}], [u_1, r_{NO}]. The first mode (ϕ) has been contracted (see Section IIIB in Ref.[16]).

DOF	**DVR**	**N**	**Range**
r_{OH}	HO	18	[1.30, 2.45]
r_{NO}	HO	13	[1.90, 2.60]
u_2	HO	13	[-0.65, -0.10]
r_{ON}	HO	16	[2.10, 3.25]
u_1	HO	18	[-0.65, 0.25]
ϕ	cos	32	[0, $2\pi/2$]

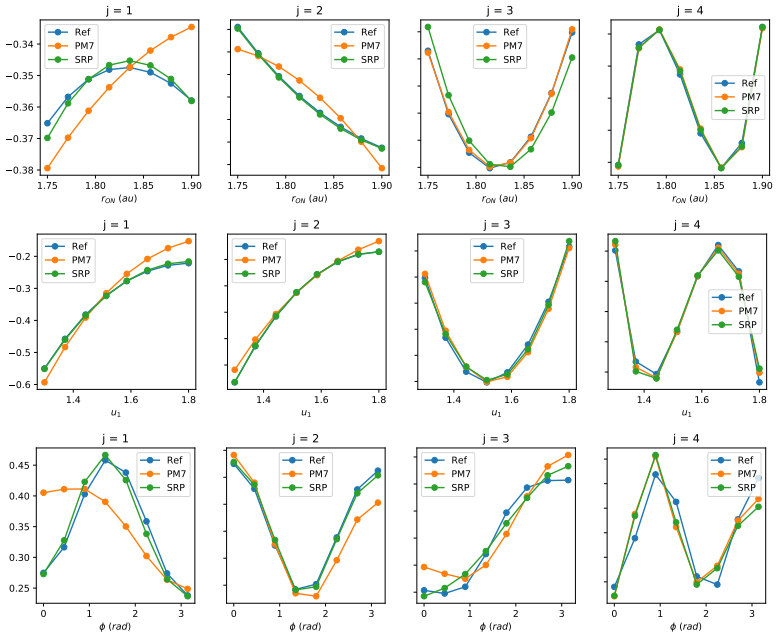

FIG. 7: First four SPPs for the r_{NO}, u_1, and ϕ DOF (see Figure 6 and Table IV) in the HONO molecule obtained by HOOI Tucker decomposition using (i) the reference potential by Richter *et al.*[61] (ii) the Parametric Model 7 (PM7) Hamiltonian[57] and (iii) the resulting SRP.

At this point, we make use of the particular distribution of values within the *core* tensor. The latter could be understood to play a role analogous to that of configuration interaction coefficients in electronic structure. First of all, it should be noticed that these values span a huge energy interval from 10^7 down to 10^{-6} (values in cm$-$1). The maximum corresponds to 22646896 cm$-$1 and 6940 cm$-$1 is the mean value. Second, a large fraction of the total number of coefficients lies between $[10^{-2}, 10^{-3}]$ and almost the half of them lie below 10^{-2}. Considering this particular distribution and this huge span of values, we can safely consider consider the *core* tensor as being *effectively* sparse. In other words, the relative weight of a large fraction of the configurations is negligible. We can profit from this fact and assign zero value to all the elements below a certain threshold. This, in turn, implies a dramatic reduction in the dimension of the SOP-FBR configuration space, thus leading to a higher efficiency and a more compact SOP-FBR final expression.

TABLE V: Analysis of the [5, 5, 5, 5, 5, 12] *core* tensor values for HONO (see main text for the discussion). The total number of tensor elements is N=37500, n is the number of *core* elements below a certain threshold value (Thrs) in cm^{-1}. In the last column, we define an *effective* sparsity as ((N-n)/N) in percentage.

Thrs	**n**	**N-n**	**(N-n)/N**
10^{+7}	37499	1	0.00
10^{+6}	37495	5	0.00
10^{+5}	37409	91	0.00
10^{+4}	37000	500	1.33
10^{+3}	36165	1335	3.56
10^{+2}	34834	2666	7.11
10^{+1}	33105	4395	11.72
10^{-0}	31225	6275	16.73
10^{-1}	28661	8839	23.57
10^{-2}	20041	17459	46.56
10^{-3}	3650	33850	90.27
10^{-4}	402	37098	98.93
10^{-5}	36	37464	99.90
10^{-6}	5	37495	99.99

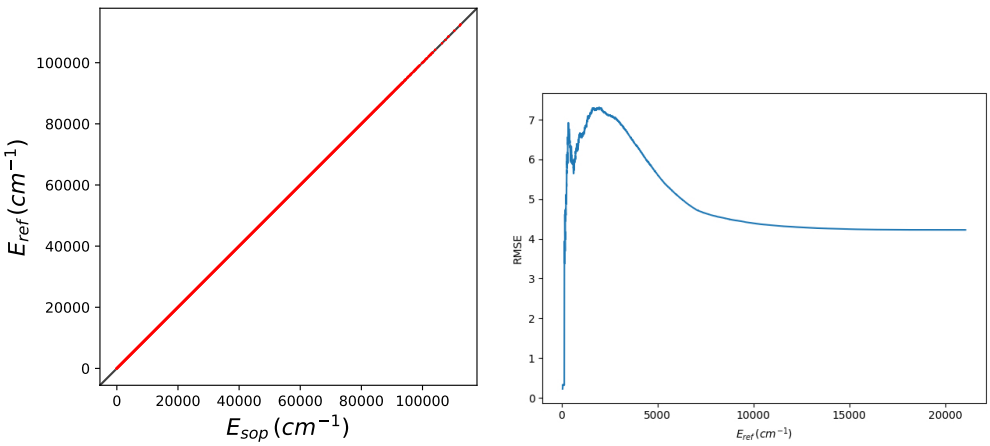

FIG. 8: Correlation plot between the reference *ab initio* energies and corresponding SOP-FBR energies, and cumulative RMSE values.

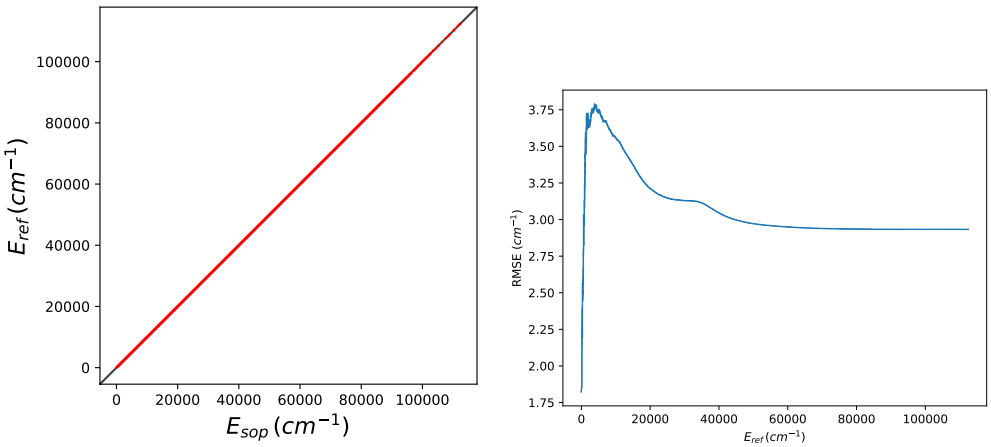

FIG. 9: Correlation plot between the reference *ab initio* energies and corresponding HOOI energies, and cumulative RMSE values.

To carefully assess the quality of our SOP-FBR PES, we have used a validation set consisting on 10^6 points generated in the form of a grid within the same boundaries as our reference but much denser. In addition to this, in order to assess/identify possible errors associated to the SOP-FBR form, we have performed an extra set of calculations using directly the HOOI decomposition of the original PES and having it transformed into SOP-FBR form (Chebyshev expansion of the basis).

The SOP-FBR RMSE was 7.22 cm^{-1}, a satisfactory value somewhat larger than the one

obtained for HOOI (2.93 cm^{-1}). The former value should be understood in the context of a direct fit from *ab initio* points, that is, it should be compared to the RMSE obtained for the reference PES of about 5 cm^{-1}.[61] The reliability of the SOP-FBR has been also assessed with a validation set consisting in 10^6 points for which we obtained an RMSE of 11.85 cm^{-1}. Analogously, the same calculation for the HOOI yielded a value of 4.20 cm^{-1}. It should be noticed that the ratio between the RMSEs in the validation and reference sets is about 1.5 for both SOP-FBR and HOOI.

In Figure 8, we provide a graphical representation for these calculations. It can be observed that for the whole range of fitted energies [0, 100000] cm^{-1} a nice agreement between the reference and SOP-FBR values is obtained. At this point, it should highlighted that we have tackled a range of energies ten times higher than previous studies dealing with the same system.[32] The SOP-FBR optimisation required 0.37 hours of CPU using 12 processors.

As an extra test of quality, we have also characterised the stationary points of the SOP-FBR PES. For this, we have computed the *cis* and *trans* minima as well as the corresponding transition state using a steepest descent algorithm in reduced dimensionality: we have enforced the torsion angle at the corresponding reference value, optimise the remaining coordinates and assess the resulting gradient. In all cases, the maximum value of the gradient did not exceed 10^{-7} units. The resulting geometrical parameters are presented in Table VI. As in the case of the water molecule, we obtain values that agree up to the fourth decimal place for both distances and angles.

TABLE VI: Comparison of the coordinate values of the stationary points (*trans*- and *cis*-minima and *cis-trans* transition state, TS) for the reference PES and the SOP-FBR PES. Geometries obtained with the steepest descent algorithm by imposing the reference torsion angle. In all cases, the maximum component of the gradient (in absolute value) lies below 10^{-7} units (all values are in fact between 10^{-7} and 10^{-10}). Distances are given in atomic units and angles in radians.

	Coordinate					
PES	$\mathbf{r_{NO}}$	$\mathbf{r_{ON}}$	$\mathbf{r_{OH}}$	$\boldsymbol{\theta_2}$	$\boldsymbol{\theta_1}$	$\boldsymbol{\phi}$
			trans			
Ref.	2.6965	1.8224	2.2129	1.7773	1.9312	3.1416
SOP-FBR	2.6967	1.8231	2.2133	1.7777	1.9315	3.1416
			cis			
Ref.	2.6314	1.8411	2.2369	1.8218	1.9746	0.
SOP-FBR	2.6305	1.8412	2.2374	1.8224	1.9753	0.
			TS			
Ref.	2.8475	1.8178	2.2008	1.7575	1.9290	1.5080
SOP-FBR	2.8475	1.8179	2.2009	1.7578	1.9288	1.5080

The reliability of our SOP-FBR can be further illustrated by noticing its *variational* behaviour. In Table VII, we present the RMSE computed on the reference primitive grid (Table IV) for trimmed SOP-FBR expansions (*cf.* td-MGPF[16]) As it can be observed, the results compare well (and even improve) those of POTFIT (from Table IV in Ref.[16]) thus confirming the possibility of numerically *strolling* towards different (and sometimes more favourable) minima than POTFIT (or HOOI) in Tucker configuration space. Interestingly, the SOP-FBR *Schmidt* functions are orthonormal as in POTFIT or MGPF.

As definitive test of the quality of our SOP-FBR PES, we have computed its ZPE and the 20 lowest vibrationally excited eigenvalues. With respect to the ZPE, our value is of 4366.7 cm^{-1} which nicely compares to the reference one of 4367.7 cm^{-1} and fully agrees with the HOOI one (4365.5 cm^{-1}). In Table VIII, we provide a comparison of the results for SOP-FBR, HOOI and the reference PES (exact). As it can be observed, there is a nice agreement among the three sets. There is slight misestimate (common to both SOP-FBR and HOOI)

TABLE VII: Analysis of the RMSE for trimmed SOP-FBR (FBR) expansions starting from the [5, 5, 5, 5, 5, 12] (see main text for the discussion). The RMSE units are meV for the sake of comparison with POTFIT (PF) results obtained from Ref.[16].

		Error	
SPPs	**Terms**	**FBR**	**PF**
$[3, 3, 3, 3, 3, c]$	243	20.84	131.68
$[4, 4, 3, 4, 4, c]$	768	5.05	34.06
$[4, 4, 4, 4, 4, c]$	1024	3.39	21.46
$[5, 5, 5, 5, 5, c]$	3125	1.93	0.75

of certain eigenvalues associated to the *cis* well,[61] whose origin can safely attributed to the sampling of this particular region.

TABLE VIII: Comparison of the 20 lowest vibrational eigenvalues of HONO for the original PES, the HOOI, and the SOP-FBR one. The first column indicates the label of the state and its character: c, *cis*-well and t, *trans*-well.

State	**Eigenenergies (cm^{-1})**		
	SOP-FBR	**HOOI**	**Reference**
0	0.0	0.0	0.0
1c	91.2	98.5	94.1
2t	600.7	600.6	600.8
3c	707.8	715.0	710.7
4t	795.7	795.7	795.9
5c	941.2	948.5	944.1
6t	1055.3	1055.2	1055.4
7t	1187.8	1187.6	1188.1
8t	1264.5	1264.4	1264.9
9c	1300.1	1310.4	1306.6
10c	1309.8	1317.0	1312.8
11t	1385.1	1385.0	1385.3
12c	1401.4	1408.8	1404.8
13c	1544.8	1552.9	1547.9
14t	1574.5	1574.6	1574.9
15t	1640.7	1640.4	1640.9
16t	1689.7	1689.8	1689.9
17c	1723.0	1730.1	1726.0
18t	1762.4	1762.1	1762.4
19c	1776.6	1783.7	1779.7
20t	1828.7	1828.5	1829.0

IV. DATA AVAILABILITY

The data that support the findings of this study are available from the corresponding author upon reasonable request.

V. CONCLUSIONS

We have presented sum-of-products Finite Basis Representation (SOP-FBR), an algorithm that yields a PES in Tucker form directly from a set of reference *ab initio* points. In SOP-FBR, the Schmidt basis (*aka* SPPs in the MCTDH literature) are expressed in terms of a weighted sum of orthonormal polynomials. The Schmidt basis are universal for the same type of PES and enclose in a non-evident way the topography of the PES (correlation among different DOF). The SOP-FBR expression is analytical and differentiable *ad infinitum* and as such, SOP-FBR is ideally suited for its use in (classical or semi-classical) dynamical simulations. More specifically, SOP-FBR allows for a seamlessly interfacing with quantum dynamical codes such as MCTDH[62] or Quantics.[63] We have shown that the SOP-FBR can be straightforwardly symmetrized by *ansatz* thus diminishing the computational cost of the algorithm. In addition to this, we have also profited from the sparse character of the Tucker *core* tensors. The quality and smoothness of the SOP-FBR PES has been extensively benchmarked against reference potentials (both model and high-level *ab initio* PES) by carefully analysing the different errors (RMSE, correlation plots, cumulative RMSE) as well as by comparing the resulting vibrational eigenvalues of each PES. We have observed that SOP-FBR can lead to Tucker expansions which are *more optimal* than those obtained by an equivalent POTFIT (or related methods). The current (beta) version of the SOP-FBR code has been written in Python 3.8.5 and will be freely distributed upon request. The implementation has been interfaced with the Heidelberg MCTDH software package.[62]

VI. SUPPLEMENTARY MATERIAL

The full list of coefficients corresponding to the SOP-FBR PES for H_2O and HONO are available in the Supplementary Material file. Energies are given in cm^{-1}. In each list, the first two lines present (1) the core dimensions (same as the number of DOF) and (2) the number of Chebyshev functions per dimension, respectively. The rest of the lines

present the Chebyshev expansion coefficients and the core tensor elements in a column-major (colexicographic) ordering.

VII. ACKNOWLEDGEMENTS

The authors would like to thank Hans-Dieter Meyer and Markus Schröder (Heidelberg) for fruitful and sustained discussions. The authors would also like to thank Tucker Carrington (Queen's) for his careful reading of the original version of the manuscript and his thoughtful comments. RLPB thanks the Région Hauts-de-France and the Université de Lille for a Ph.D. Fellowship. The authors gratefully acknowledge the computational support of Valérie Vallet and Florent Réal (Lille) and Andrei Borissov (Paris-Saclay). The authors acknowledge the usefulness Reviewers' comments and suggestions that have helped improving this manuscript. Finally, RLPB would like to especially thank Jimmy Aguilar Mena (BSC-CNS) for fruitful discussions on Computer Science related aspects.

---

[1] M. H. Beck, A. Jäckle, G. A. Worth, and H.-D. Meyer, Phys. Rep **324**, 1 (2000).

[2] H. Wang and M. Thoss, J. Chem. Phys. **119**, 1289 (2003).

[3] U. Manthe, J. Chem. Phys. **128**, 164116 (2008).

[4] O. Vendrell and H.-D. Meyer, J. Chem. Phys. **134**, 044135 (2011).

[5] S. Römer, M. Ruckenbauer, and I. Burghardt, J. Chem. Phys. **138**, 064106 (2013).

[6] G. W. Richings, I. Polyak, K. E. Spinlove, G. A. Worth, I. Burghardt, and B. Lasorne, Int. Rev. Phys. Chem. **34**, 269 (2015).

[7] P. S. Thomas, T. Carrington, J. Agarwal, and H. F. Schaefer, J. Chem. Phys. **149**, 064108 (2018).

[8] D. Mendive-Tapia, E. Mangaud, T. Firmino, A. de la Lande, M. Desouter-Lecomte, H.-D. Meyer, and F. Gatti, J. Phys. Chem. B **122**, 126 (2018).

[9] V. Baranov and I. Oseledets, J. Chem. Phys. **143**, 174107 (2015).

[10] H. R. Larsson, J. Chem. Phys. **151**, 204102 (2019).

[11] S. M. Greene and V. S. Batista, J. Chem. Theory Comput. **13**, 4034 (2017).

[12] N. DeGregorio and S. S. Iyengar, J. Chem. Theory Comput. **15**, 2780 (2019).

[13] F. Gatti, C. Iung, M. Menou, Y. Justum, A. Nauts, and X. Chapuisat, J. Chem. Phys. **108**, 8804 (1998).

[14] D. Lauvergnat and A. Nauts, J. Chem. Phys. **116**, 8560 (2002).

[15] A. Jäckle and H.-D. Meyer, J. Chem. Phys. **104**, 7974 (1996).

[16] D. Peláez and H.-D. Meyer, J. Chem. Phys. **138**, 014108 (2013).

[17] M. Schröder and H.-D. Meyer, J. Chem. Phys. **147**, 064105 (2017).

[18] F. Otto, J. Chem. Phys. **140**, 014106 (2014).

[19] F. Otto, Y.-C. Chiang, and D. Peláez, Chem. Phys. **509**, 116 (2018).

[20] R. L. Panadés-Barrueta, E. Martínez-Núñez, and D. Peláez, Front. Chem. **7**, 576 (2019).

[21] G. W. Richings and S. Habershon, J. Chem. Phys. **148**, 134116 (2018).

[22] B. J. Braams and J. M. Bowman, Int. Rev. Phys. Chem. **28**, 577 (2009).

[23] R. Dawes, D. L. Thompson, Y. Guo, A. F. Wagner, and M. Minkoff, J. Chem. Phys. **126**, 184108 (2007).

[24] C. Sanz-Sanz, O. Roncero, M. Paniagua, and A. Aguado, J. Chem. Phys. **139**, 184302 (2013).

[25] T. Frankcombe and M. Collins, Phys. Chem. Chem. Phys. **13**, 8379 (2011).

[26] B. Jiang, J. Li, and H. Guo, International Reviews in Physical Chemistry **35**, 479 (2016).

[27] O. T. Unke, D. Koner, S. Patra, S. Käser, and M. Meuwly, Mach. Learn.: Sci. Technol. **1**, 013001 (2020).

[28] V. Barone, J. Chem. Phys. **122**, 014108 (2005).

[29] R. Ramakrishnan and G. Rauhut, J. Chem. Phys. **142**, 154118 (2015).

[30] L. Barnes, B. Schindler, I. Compagnon, and A.-R. Allouche (2017), 1704.02144.

[31] S. Manzhos and T. Carrington, Jr., J. Chem. Phys. **125**, 084109 (2006).

[32] E. Pradhan and A. Brown, Phys. Chem. Chem. Phys. **19**, 22272 (2017).

[33] B. Jiang and H. Guo, J. Chem. Phys. **141**, 034109 (2014).

[34] F. Richter, P. Carbonniere, A. Dargelos, and C. Pouchand, J. Chem. Phys. **136**, 224105 (2012).

[35] P. S. Thomas, M. F. Somers, A. W. Hoekstra, and G. J. Kroes, Phys. Chem. Chem. Phys. **14**, 8628 (2012).

[36] F. Richter, P. Carbonniere, and C. Pouchan, J. Chem. Phys. **114**, 1401 (2014).

[37] G. Ávila and T. Carrington, J. Chem. Phys. **143**, 044106 (2015).

[38] A. Aerts, P. Carbonniere, F. Richter, and A. Brown, J. Chem. Phys. **152**, 024305 (2020).

[39] M. Schröder, J. Chem. Phys. **152**, 024108 (2020).

[40] L. D. Lathauwer, B. D. Moor, and J. Vandewalle, SIAM Journal on Matrix Analysis and Applications **21**, 1253 (2000).

[41] J. D. Carroll and J. J. Chang, Psychometrika **35**, 283 (1970).

[42] R. A. Harshman, UCLA Working Papers in Phonetics **16**, 1 (1970).

[43] T. G. Kolda and B. W. Bader, SIAM Review **51**, 455 (2009).

[44] V. K. B. N. Khoromskij, Central European Journal of Mathematics **5**, 523 (2007).

[45] J. Kossaifi, Y. Panagakis, A. Anandkumar, and M. Pantic, J. Mach. Learn. Res. **20**, 925 (2019), ISSN 1532-4435.

[46] S. Manzhos and T. Carrington, Jr., J. Chem. Phys. **125**, 084109 (2006).

[47] D. Peláez, K. Sadri, and H.-D. Meyer, Spectrochimica Acta part A **119**, 42 (2014).

[48] D. Peláez and H.-D. Meyer, Chem. Phys. **482**, 100 (2017).

[49] A. Haller, D. Peláez, and A. Bande, J. Phys. Chem. C **123**, 14754 (2019).

[50] M. Nest and H.-D. Meyer, J. Chem. Phys. **117**, 10499 (2002).

[51] D. Wales and J. P. K. Doye, J. Phys. Chem. A **101**, 5111 (1997).

[52] P. Virtanen, R. Gommers, T. E. Oliphant, M. Haberland, T. Reddy, D. Cournapeau, E. Burovski, P. Peterson, W. Weckesser, J. Bright, et al., Nature Methods **17**, 261 (2020).

[53] J. Nocedal and S. J. Wright, *Numerical optimization* (Springer, Heidelberg, 2006).

[54] O. L. Polyansky, P. Jensen, and J. Tennyson, J. Chem. Phys. **105**, 6490 (1996), pES, water.

[55] R. L. Panadés-Barrueta and D. Peláez, *SRPTucker software package* (2019).

[56] J. J. P. Stewart, `HTTP://OpenMOPAC.net` (2016).

[57] J. J. P. Stewart, J. Mol. Model. **19**, 1 (2013).

[58] A. H. G. Kan and G. T. Timmer, Math. Program. **39**, 57 (1987).

[59] M. J. D. Powell, Cambridge NA Report NA2009/06, University of Cambridge pp. 26–46 (2009).

[60] S. Kopec, E. Martínez-Núñez, J. Soto, and D. Peláez, Int. J. Quant. Chem. p. e26008 (2019).

[61] F. Richter, M. Hochlaf, P. Rosmus, F. Gatti, and H.-D. Meyer, J. Chem. Phys. **120**, 1306 (2004).

[62] G. A. Worth, M. H. Beck, A. Jäckle, and H.-D. Meyer, The MCTDH Package, H.-D. Meyer, Version 8.4.12. See http://mctdh.uni-hd.de/ (2016).

[63] G. A. Worth, K. Giri, G. W. Richings, I. Burghardt, M. H. Beck, A. Jäckle, and H.-D. Meyer, The QUANTICS Package, Version 1.1, See https://www2.chem.ucl.ac.uk/worthgrp/quantics/doc/quantics/citation.html/ (2015).